Nat. Hazards Earth Syst. Sci. Discuss., https://doi.org/10.5194/nhess-2017-252
Manuscript under review for journal Nat. Hazards Earth Syst. Sci.
Discussion started: 22 September 2017

Natural Hazards and Earth System Sciences
Discussions

Wave run-up prediction and observation in a micro-tidal beach

Diana Di Luccio[1], Guido Benassai[2], Giorgio Budillon[1], Luigi Mucerino[3], Raffaele Montella[1], and Eugenio Pugliese Carratelli[4]

[1]University of Naples "Parthenope", Science and Technologies Department, Centro Direzionale Is. C4, 80143 Napoli, Italy
[2]University of Naples "Parthenope", Engineering Department, Centro Direzionale Is. C4, 80143 Napoli, Italy
[3]University of Genova, Department of Earth, Environment and Life Sciences, Corso Europa 26, 16132 Genova, Italy
[4]Inter-University Consortium for the Prediction and Prevention of Major Risks Hazards (CUGRI), 84080 Penta di Fisciano (SA), Italy

Correspondence to: Diana Di Luccio (diana.diluccio@uniparthenope.it)

Abstract. Extreme weather events have significant impacts on coastal human activities and related economy. In this scenario the forecast of sea storms and wave run-up events is a challenging goal to mitigate the wave effects on shores, piers and coastal structures. To do this, we used a computational model chain based on both community and ad hoc developed numerical models in an operational context to evaluate the beach inundation levels. At this aim, we compared the results of simulated and observed wave run-up levels on a micro-tidal beach located on the northern Tyrrhenian Sea. The offshore wave simulations have been performed by WaveWatch III model, implemented by Campania Center for Marine and Atmospheric Monitoring and Modelling (CCMMMA) - University of Naples Parthenope, which were used as initial conditions for run-up calculations using different formulas. The validation of the simulated waves was done with different observation systems. The offshore wave simulations were matched with remote sensing data, while the run-up levels calculated with different formulas were compared with observations taken from a video camera system. The usual statistical errors were taken as a measurement of the modelling system capability to properly simulate the beach run-up during a storm.

Keywords: model chain, wave numerical model, beach run-up, video monitoring.

1 Introduction

The monitoring and the forecasting of wind wave interaction processes become particularly critical along the coastal areas, which are highly dynamically and morphologically complex systems that respond in a nonlinear manner to external perturbations, giving rise to coastal vulnerability (Didenkulova, 2010; Di Paola et al., 2014)), and coastal risk due to sea level rise (Benassai et al. (2015a)) and subsidence (Aucelli et al. (2016)). The main damages caused by extreme wave events are due to sea waves hitting infrastructures, such as beach resorts that are kept on the beach also during the winter season (Casella et al. (2014)). Based on this rationale, the evolution of winds, waves and the wind-driven sea circulation is of great applicative relevance for both the modelling and the forecasting of the wave climate (Bertotti and Cavaleri, 2009; Cavaleri and Rizzoli, 1981; Mentaschi et al., 2013; Benassai and Ascione, 2006a) and the observation of oceanographic phenomena (Bidlot et al. (2002)). The wind wave simulations critically depend on the quality of the driving wind fields (Rusu et al. (2014)), which are provided by forecasting and/or climatological winds or alternatively by active satellite-based microwave Synthetic Aperture

Nat. Hazards Earth Syst. Sci. Discuss., https://doi.org/10.5194/nhess-2017-252
Manuscript under review for journal Nat. Hazards Earth Syst. Sci.
Discussion started: 22 September 2017

Natural Hazards and Earth System Sciences Discussions

Radar (SAR) (Johannessen and Bjorgo (2000)). The comparison between the wave simulations obtained by these different data source have been demonstrated the capability of the SAR-based wind field retrieval to improve coastal wind wave modelling (Benassai et al., 2013a, b, 2015b). With regard to coastal zone monitoring, the coastal evolution can be surveyed by remote sensing acquisition (Nunziata et al. (2016)), while shorter time scale beach processes can be observed by UAV (Benassai et al. (2017)) and video monitoring system (Brignone et al. (2012)).

In particular, wave run-up prediction is required in most coastal vulnerability and risk evaluation projects (Didenkulova and Pelinovsky, 2008; Didenkulova et al., 2010). Despite a number of available numerical models (Dodd, 1998; Hubbard and Dodd, 2002) gives accurate estimates of wave run-up for given boundary conditions, simplified run-up formulas are useful to give realistic results on existing cross-shore profiles. The earliest formulation of run-up height was by (Hunt (1959)) who calculated run-up from incident regular waves. Later research included irregular waves and obtained statistical values of the run-up levels, that is Ru_{max} (the highest run-up height during each run), $Ru_{2\%}$ (the 2% excess run-up height), $Ru_{10\%}$ (the average of the highest one-tenth of the total run-up heights), $Ru_{33\%}$ (the one-thirds highest run-up height), Ru_{mean} (the average of the total run-up heights). Mase (1989) introduced two coefficients which were dependent on the characteristic run-up level $Ru_{x\%}$, as defined in section 3.2. Stockdon et al. (2006) considered the run-up level $Ru_{2\%}$ as a function of the two different contributions of wave set-up and swash.

In this paper we computed the wave run-up levels with the previous different formulations to obtain run-up time series. Since no actual local measurements from buoys were available (Montella et al. (2008)), calculations from WaveWatch III (WW3) wave model were used instead by means of a high spatial resolution weather-ocean forecasting system implemented by Campania Center for Marine and Atmospheric Monitoring and Modelling (CCMMMA) - University of Naples "Parthenope", using a high performance computing (HPC) system for simulation and open environmental data dissemination (Montella et al. (2007)). The deep water numerical models (Ascione et al. (2006)) were integrated with a wave propagation model in shallow water and the consequent run-up evaluation on the beach. This model was operationally implemented for a micro-tidal beach located on the northern Tyrrhenian Sea, in order to test the reliability of the wave modelling system, already verified in offshore conditions by in situ and remote sensing techniques (Carratelli et al., 2007; Reale et al., 2014; Benassai and Ascione, 2006b) also on the simulation of the beach processes. To do this, the run-up levels associated with a typical one-year return period storm were compared with the ones observed by a video camera system. To this aim, the offshore wave simulations were previously validated with remote sensing data (as already done by (Montuori et al., 2011; Benassai et al., 2012)) and then used to initial conditions for run-up calculations using different formulas. The obtained run-up levels on the beach were validated with observations by camera system using timestack images. The whole procedure demonstrated the capability of the modelling system to properly simulate the beach processes during a storm.

Innovation: At the best of our knowledge, in recent years, a number of papers has been published on offshore validation of numerical simulation models, as well as on the nearshore validation of run-up formulas, but very few on a global verification of an operational model chain which starts from the forecasted wind till wave and run-up calculation on the beach.

The paper is organized as follows: the numerical models and the field data are reported in chapter 2, the simulation results and

Nat. Hazards Earth Syst. Sci. Discuss., https://doi.org/10.5194/nhess-2017-252
Manuscript under review for journal Nat. Hazards Earth Syst. Sci.
Discussion started: 22 September 2017

Natural Hazards and Earth System Sciences
Discussions

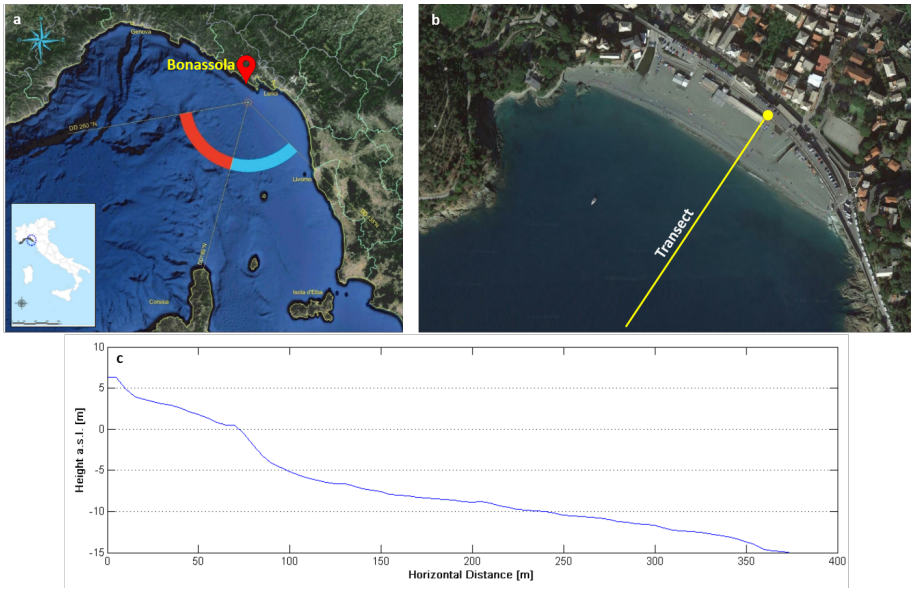

Figure 1. Bonassola beach. Red line shows investigated profile and graph draws morphodynamic features. Yellow circle represents camera system location

the comparison with field data are given in chapters 3 and finally, the discussion and the conclusion are reported in chapter 5 and 6, respectively.

2 Study area and wave climate

Test case presented in this work was carried out on Bonassola beach (La Spezia, Italy), which is located on the eastern coast of Liguria. The beach, about 410 m long, does not include defense structures. The Bonassola coast is oriented South-East/North-West, so it is exposed to waves coming from South-West (215°-245°), while it is protected by the South-East waves. This gravel beach has steep and typically concave profiles with slope increasing up to the beach face. The mean beach slope is approximately 8.3% from the shoreline to 10m water depth and becomes 5.5% between 10 and 30m (Fig. 1c). The offshore beach is composed by mean and coarse sand.

The potential exposure to the waves can be defined by identifying the main and secondary fetches. The main fetch is limited by the directions 195°N and 260°N, while the secondary fetch is limited between the directions 135°N and 195°N (in the following S_1).

In order to analyze the extreme sea events, the offshore wave climate was extracted using the data recorded by Italian SWAN (Sea WAve measurement Network) buoy located offshore La Spezia (43°55'41.99"N 09°49'36.01"E) since year 1989 till 2014. The main transverse sector was later subdivided into two sub-sectors, 195-225°N (S_2) and 225-260°N (S_3), in which we detected two different wave conditions: maximum H_s lower than 5.5 m between 195°N and 225°N and higher than 5.5m

Nat. Hazards Earth Syst. Sci. Discuss., https://doi.org/10.5194/nhess-2017-252
Manuscript under review for journal Nat. Hazards Earth Syst. Sci.
Discussion started: 22 September 2017

Natural Hazards and Earth System Sciences
Discussions

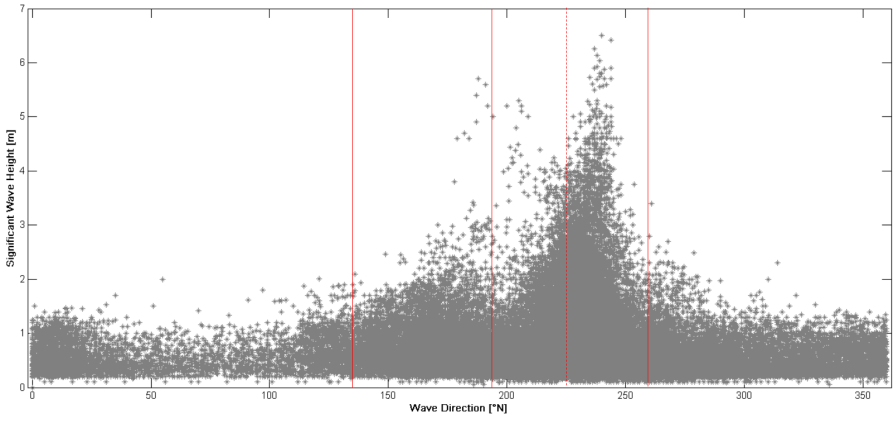

Figure 2. Significant wave heights and wave directions recorded from the SWAN buoy of La Spezia 1989-2009.

between 225°N and 260°N (Fig. 2). The H_s time series was processed to obtain the extreme sea storm events. In order to obtain a statistically significant time series, a representative sample of extreme statistically independent wave events N have been selected on the basis of the Peak Over Threshold method (Goda (1989)). The 48h-maxima based on over-threshold H^* time series has been sorted in order to find the best fit between the data and the Gumbel (Fisher-Tippet I) cumulative probability distribution function.

$$P(H) = e^{-e^{-\left(\frac{H-B}{A}\right)}} \tag{1}$$

where A is the location parameter and B is the scale parameter. A rank index m, ranging from 1 to N was associated to order the array and the sample rate of non-exceedance $F(H_s<H^*)$ was calculated as

$$F(H_s) < H^* = 1 - \frac{m - 0.44}{N + 0.12} \tag{2}$$

and it is assumed coincident with the non exceedance probability.

$$y_m = -ln[-lnF(H_s < H^*)] \tag{3}$$

Figure 3 shows the rate between $H_s<H^*$ and relative reduced variable for waves coming from each directional sector.

The linear regression line y=ax+b is given as

$$H_s = Ay_m + B \tag{4}$$

where A (slope of the regression line) and B (line intercept) coefficients are linked with the probability distribution function. The wave heights for different return periods can be determined by the following expressions:

$$H_r = Ay_r + B \tag{5}$$

Nat. Hazards Earth Syst. Sci. Discuss., https://doi.org/10.5194/nhess-2017-252
Manuscript under review for journal Nat. Hazards Earth Syst. Sci.
Discussion started: 22 September 2017

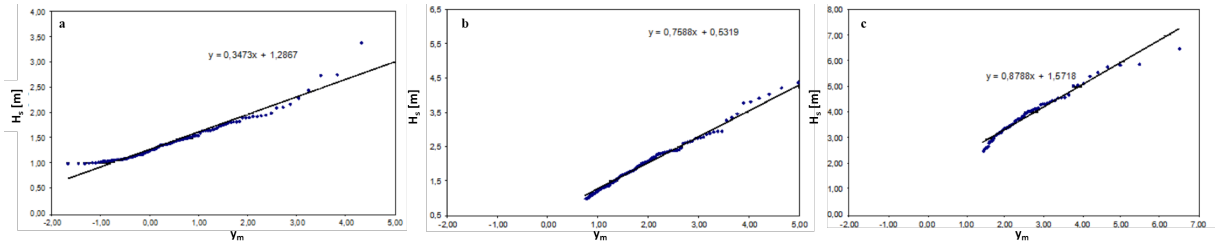

Figure 3. Matching between the recorded extreme wave heights and the reduced variable for Gumbel distribution function for waves coming from a) 135°N-195°N; b) 195°N-225°N; c) 225°N-260°N.

Table 1. Design waves obtained from La Spezia buoy (1989-2009) for different return periods an each directional sector.

T_r	Sector	H_r	y_r	T_r	Sector	H_r	y_r
	S_1	2.84	4.46		S_1	3.88	7.46
1	S_2	3.72	4.20	20	S_2	6.00	7.21
	S_3	5.59	4.57		S_3	8.23	7.57
	S_1	3.40	6.08		S_1	4.20	8.38
5	S_2	4.95	5.82	50	S_2	6.70	8.12
	S_3	7.01	6.19		S_3	9.03	8.49
	S_1	3.64	6.77		S_1	4.44	9.07
10	S_2	5.74	6.51	100	S_2	7.22	8.82
	S_3	7.62	6.88		S_3	9.4	9.18

where H_r is the significant wave height with return period T_r and the relative reduced variable is

$$y_r = -ln\left[-ln\left(1-\frac{1}{\lambda T_r}\right)\right] \quad (6)$$

and the sample intensity λ is defined by the ratio between the number of extreme events and the number of years of observation. Table 1 gives the offshore wave heights obtained for each directional sector as functions of the relative return period T_r, which are maximum for the western directions (sector S_3), with H_s>5.0m.

In order to evaluate the wave run-up levels associated to frequent wave conditions, we chose a recent wave storm coming from western directions with significant wave heights that can occur several times a year (that is with a return period lower than one year). For this storm numerical simulations, performed with WW3 model were accomplished with run-up calculations using different empirical formulas.

Nat. Hazards Earth Syst. Sci. Discuss., https://doi.org/10.5194/nhess-2017-252
Manuscript under review for journal Nat. Hazards Earth Syst. Sci.
Discussion started: 22 September 2017

3 Methods

3.1 Wave numerical simulations

The weather/sea forecasting tool in Fig. 4, implemented by CCMMMA hosted by the University of Naples "Parthenope", has been configured using an HPC infrastructure to manage and run a modeling system based on the algorithms implemented in the open-source numerical models Weather Research and Forecasting (WRF) (Skamarock et al. (2001)) and WavewatchIII (WW3) (Tolman et al. (2009)) organized in a workflow. The actually operational system is based on complex data acquisition, processing, simulation, post-processing and intercomparison dataflow, provided by FACE-IT workflow engine (Pham et al. (2012)), available as open source and cloud service. This integrated data processing and simulation framework enables: i) the data ingest from geospatial archives; ii) the data regridding, aggregation, and other processing prior to simulation; iii) the leveraging of the high-performance and cloud computing; iv) the post-processing to produce aggregated yields and ensemble variables needed for statistics and model testing. The main workflow tool is the WRF numerical model which gives the 10 m wind fields atmospheric forcing needed to drive WW3 model for estimating the offshore waves, which is the initial and boundary conditions for the modeling of waves in shallow water and run-up/overtopping calculator software.

Wave simulations were carried out using the WW3 model (Tolman and Chalikov (1996)), a third generation wave model developed at NOAA/NCEP. In this paper, WW3 model computational domain was configured as 486x353 grid points and 0.09° spatial resolution in latitude (Lat_{min}=6.33°N, Lat_{max}=20.88°N) and in longitude (Lon_{min}=36.42°E, Lon_{max}=46.98°E). Outputs from the model include gridded fields with the associated significant wave height (H_s), wave direction (Dir_{mn}), mean period (T_m) and spectral information. The WW3 grid points close to the coast were used as "virtual buoys" (VB) to compute the wave transformation down to the coast, with the final goal of simulating the run-up parameter on the beaches.

3.2 Wave run-up calculator

Since Hunt (1959), who used regular waves, the wave run-up Ru, defined as the vertical elevation above the still water level, has been expressed as:

$$\frac{Ru}{H_0} = \xi \tag{7}$$

where ξ is the Iribarren number or surf similarity parameter (Battjes (1975))

$$\xi = \frac{tan\beta}{\sqrt{\frac{H_0}{L_0}}} \tag{8}$$

and β is the beach slope angle, H_0 is the deepwater significant wave height and L_0 is the linear theory deep-water wavelength (Airy (1841))

$$L_0 = \frac{gT^2}{2\pi} \tag{9}$$

Nat. Hazards Earth Syst. Sci. Discuss., https://doi.org/10.5194/nhess-2017-252
Manuscript under review for journal Nat. Hazards Earth Syst. Sci.
Discussion started: 22 September 2017

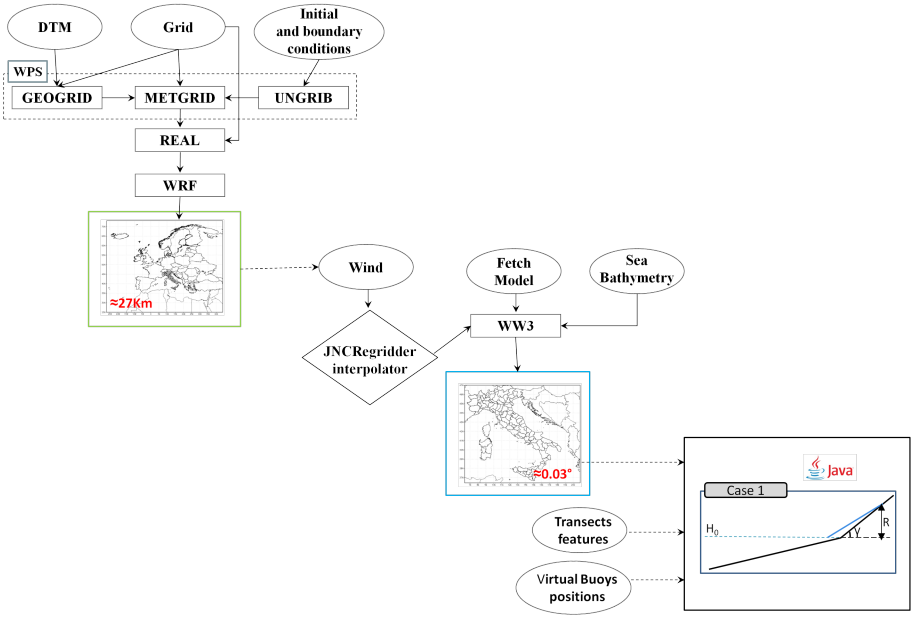

Figure 4. Model chain with the input/output data flux in the model coupling. The case 1 is the implemented run-up model calculator.

where T is the wave period. In detail, H_0 depends on the relation between the VB (C_{VB}=L_{VB}/T_m) and the deep water (C_0=L_0/T_m) (Shore Protection Manual (1984)) wave celerity:

$$H_0 = H_s \frac{C_{VB}}{C_0} \tag{10}$$

In VB the wavelength is equal to L_{VB}=(2π)/k in which k is the wavenumber obtained by the Hunt approximation of the standard dispersion relation (Fenton and McKee (1990)):

$$(kd)^2 = \left(\frac{\sigma^2 d}{g}\right)^2 + \frac{\left(\frac{\sigma^2 d}{g}\right)}{1 + \sum_{n=1}^{\infty} d_n \left(\frac{\sigma^2 d}{g}\right)^n} \tag{11}$$

where the d_n are six constant values given by Fenton, and σ is the wave frequency. The beach slope is dynamically calculated by taking into to account the profile for each coastal transect considered. The extent of flooding and the corresponding hazard level depends on the beach slope and the run-up parameter.

Holman (1986) proposed an empirical formula to obtain $Ru_{2\%}$, based on Iribarren number ξ_f constrained with surf zone slope angle.

$$\frac{Ru_{2\%}}{H_0} = 0.83\xi_f + 0.2 \tag{12}$$

Mase (1989) on the basis of laboratory tests obtained by the characteristic run-up level x as a foundation of two empirical coefficients a and b.

$$\frac{Ru_{x\%}}{H_0} = a\xi^b \tag{13}$$

Nat. Hazards Earth Syst. Sci. Discuss., https://doi.org/10.5194/nhess-2017-252
Manuscript under review for journal Nat. Hazards Earth Syst. Sci.
Discussion started: 22 September 2017

Natural Hazards and Earth System Sciences Discussions

Mase suggested a=1.86 and b=0.71 for $Ru_{2\%}$, a=2.32 and b=0.77 for Ru_{max}, a=1.70 and b=0.71 for $Ru_{10\%}$, a=1.38 and b=0.70 for $Ru_{33\%}$, a=0.88 and b=0.69 to obtain Ru_{mean}.

Stockdon et al. (2006) considered the run-up $Ru_{2\%}$ as a function of the two different contributions of wave setup and swash

$$Ru_{2\%} = 1.1\left(0.35\tan\beta_f\left(H_0L_0\right)^{0.5} + \left[H_0L_0\left(0.563\tan\beta_f^2 + 0.004\right)\right]^{0.5}\right) \quad (14)$$

where the first term in brackets represents wave setup contribution, the $\beta_f{}^2$ term is for swash contribution and the 0.004 term is for infragravity contribution. This equation was used by a number of researchers to compute coastal inundation and consequently coastal vulnerability and risk (Di Paola et al., 2014; Benassai et al., 2015a). Melby et al. (2012) compared the skill of some different run-up models through some statistical measures and introduced a new statistical skill measure, described in section 3.3.2, which was used to compare different formulations for an extensive dataset. In the following, we compared the skill of different run-up equations through the departure from the observed run-up levels evaluated with video camera records. Among the different empirical formulas used to calculate the wave run-up parameters, the last three selected equations have been adopted to obtain run-up time series. In particular, Holman, Mase and Stockdon formulas have been used for the 2% wave run-up levels, while only Mase equation has been used to calculate the 10%, 33%, mean and max run-up levels.

3.3 Observations of offshore waves and beach run-up

3.3.1 Altimeter and video monitoring

The accuracy of the wave model output in offshore conditions was evaluated against remotely sensed data. The altimeter footprint along the satellite tracks provide a large spatial coverage over the entire region of the Central and Northern Tyrrhenian Sea, which cannot be accomplished by in-situ observations at fixed stations. The altimeter data was obtained from the dataset of the Ocean Surface Topography Mission (OSTM/Jason-2), launched on 20 June 2008. In this case we use the Geophysical Data Record (GDR) data with spatial resolution of 11.2 km (Along) x 5.1 km (Across). Fig. 5 shows the considered track of the OSTM/Jason2 satellite.

The beach run-up simulations by means of different equations was evaluated by means of a video monitoring system placed in the middle of Bonassola beach (Fig. 6a, b, c, d). Video recordings of run-up were made using three video cameras, installed at an elevation of about 13 m above Mean Sea Level (MSL), which allowed a complete coverage of the beach since 19 November 2015 until now. Using the geometric transformation between ground and image coordinates, the light intensity of each pixel in the cross-shore transects was digitized. Vertical run-up elevation time series were extracted from video recordings using the time-stack method (Aagaard and Holm, 1989; Holland and Holman, 1997). This methodology, giving rise to the signal reported in Fig. 6e is described in the extensive literature on coastal video monitoring (Takewaka and Nakamura, 2001; Ojeda et al., 2008; Zhang and Zhang, 2008). The run-up position at each video sample time (1 Hz) was obtained with Beachkeeper plus (Brignone et al. (2012)), a software based on Matlab algorithm to analyze the images without any a-priori information of the acquisition system itself.

Nat. Hazards Earth Syst. Sci. Discuss., https://doi.org/10.5194/nhess-2017-252
Manuscript under review for journal Nat. Hazards Earth Syst. Sci.
Discussion started: 22 September 2017

Natural Hazards and Earth System Sciences
Discussions

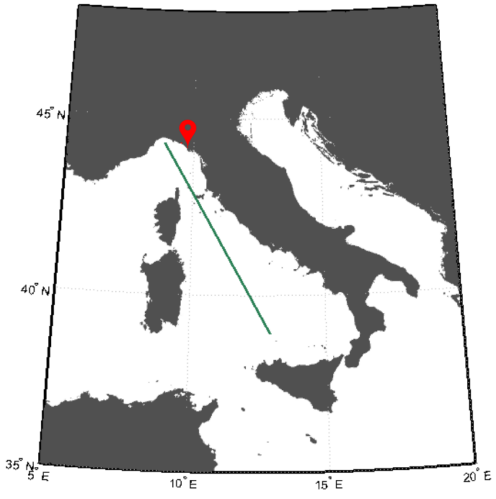

Figure 5. Map showing the position of the dataset to models testing. The green line depicts the OSTM/Jason-2 satellite dataset.

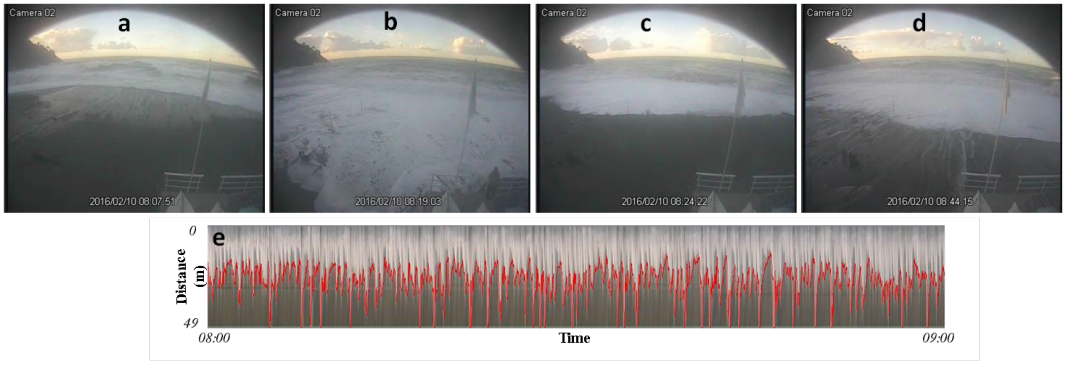

Figure 6. a) b) c) d) A time sequence of the run-up beach inundation on Bonassola beach; e) the red marker is the video camera run-up observations on Bonassola beach.

3.3.2 Comparison statistics

The quality of the results provided by the offshore wave model and by the run-up simulations was evaluated by the comparison with wave altimeter records and video-camera run-up observations. Deviation of simulated parameters from observed data was estimated through some the following statistical error indicators (S_i indicate a simulated variable, O_i indicate an observed variable and N is the number of observations):

Nat. Hazards Earth Syst. Sci. Discuss., https://doi.org/10.5194/nhess-2017-252
Manuscript under review for journal Nat. Hazards Earth Syst. Sci.
Discussion started: 22 September 2017

– the normalized Bias (BI):

$$BI = \frac{\sum_{i=1}^{N}(S_i - O_i)}{\sum_{i=1}^{N} O_i} \tag{15}$$

– the root mean square error (RMSE):

$$RMSE = \sqrt{\frac{\sum_{i=1}^{N}(S_i - O_i)^2}{N}} \tag{16}$$

– the normalized root mean square error (NRMSE):

$$NRMSE = \sqrt{\frac{\sum_{i=1}^{N}(S_i - O_i)^2}{\sum_{i=1}^{N} O_i^2}} \tag{17}$$

– the normalized scatter index (SI):

$$SI = \sqrt{\frac{\sum_{i=1}^{N}(S_i - O_i)}{\sum_{i=1}^{N} O_i^2}} \tag{18}$$

– the linear correlation coefficient (R):

$$R = \frac{cov(S_i, O_i)}{var(O_i)var(S_i)} \tag{19}$$

The results are summarized in the Summary Performance Score (SPS) index, based on the RMSE, BI and SI performance, normalized between 0 and 1.

– NRMSE Performance ($NRMSE_P$)

$$NRMSE_P = 1 - NRMSE \tag{20}$$

– BI Performance (BI_P)

$$BI_P = 1 - |BI| \tag{21}$$

– SI Performance (SI_P)

$$SI_P = 1 - SI \tag{22}$$

– Summary Performance Score (SPS)

$$SPS = \frac{NRMSE_P - BI_P - SI_P}{3} \tag{23}$$

Nat. Hazards Earth Syst. Sci. Discuss., https://doi.org/10.5194/nhess-2017-252
Manuscript under review for journal Nat. Hazards Earth Syst. Sci.
Discussion started: 22 September 2017

4 Experimental results

In this section some meaningful experimental results are presented and discussed to show the capability and accuracy of wind wave modelling chain in estimating run-up levels on the studied beach.

4.1 Offshore wave validation with altimeter data

The consistency of the WW3 model was validated taking full benefits of the ku-based altimeter data from OSTM/Jason2 mission, relative to the passage of satellite during the period from February 9th 2016 at 04:58:44 UTC to 09th 2016 at 05:00:43 UTC. Fig. 7a,b,c depicts the simulated WW3 H_s maps on February 10th 2016 at 00:00, 06:00 and 12:00 UTC, with relative zoom in Fig. 7d,e,f, respectively, while Fig. 8 shows the time history of the measured and modelled offshore H_s along the track. The results of the wind-wave modelling system were interpolated in both space and time to collocate with the altimeter data. The hourly WW3 H_s output are first spatially interpolated (bilinear interpolation) from the grid points to the locations of the altimeter measurements. Interpolations are then carried out in time to fit the satellite pass (linear time interpolation between the previous and following field values). The observed H_s is shown in blue tones in Fig. 8a, while the simulated H_s is reported in red colour (the model results are more smoothed due to minor resolution). In general, the model fits quite well the measurements, but sometimes underestimates the observations (especially the energy peaks). For example, the first high wave event between 41.5°N and 42°N is underestimated by the model, while the second high wave event between 43.5°N and 44°N is slightly overestimated.

The statistics of the comparison give an R value of 0.838, a BI of 0.192, a SI of 0.270 and a RMSE value of 0.455 m. The satisfactory agreement is shown by a RMSE lower than 0.46 m and a correlation coefficient higher than 0.83. In fact, Fig. 8 shows a good matching between simulations and observations, however it can be noted that non-negligible differences in terms of H_s are present. This could be explained by taking into account the different spatial gridding resolution scale of both modeled (WW3) and remotely sensed (Jason-2) wave estimation products.

4.2 Run-up calculation and validation with video-monitoring system

In this subsection, wave run-up numerical simulation accomplished through the operational software calculator using different empirical formulas are described with respect to the storm from February 9th-11st 2016. A preliminary offshore wave simulation has been performed on a virtual buoy located offshore Bonassola beach. The relative H_s and T_m time history has been reported in Fig. 9a, b respectively. The storm exhibits a maximum H_s higher than 3.0 m on February 10th 2016, followed by slight decrease of H_s in the following hours, with values between 2.0 m and 3.0 m.

Based on the run-up formulas described in section 3.3 on the transect described in section 2, the run-up levels are here accomplished by evaluating Ru_{mean}, $Ru_{33\%}$, $Ru_{10\%}$, $Ru_{2\%}$ and Ru_{max}. The observed wave run-up elevation time series was recorded by beach camera system along the cross transect evidenced in Fig. 1 b on February 10th 2016 from 08:00 am to 16:00 pm. Video recording of run-up (Fig. 10) were made using the central camera of the video monitoring system described in section 3.4.

Nat. Hazards Earth Syst. Sci. Discuss., https://doi.org/10.5194/nhess-2017-252
Manuscript under review for journal Nat. Hazards Earth Syst. Sci.
Discussion started: 22 September 2017

Natural Hazards and Earth System Sciences
Open Access
Discussions

Table 2. $Ru_{x\%}$ observed with cameras versus $Ru_{x\%}$ simulated using different equations.

	Simulated run-up								Observed run-up			
	Holman (1986)	Mase (1989)					Stockdon (2006)					
	$Ru_{2\%}$	$Ru_{2\%}$	$Ru_{10\%}$	$Ru_{33\%}$	Ru_{max}	Ru_{mean}	$Ru_{2\%}$	Ru_{mean}	Ru_{max}	$R_{2\%}$	$R_{10\%}$	$R_{33\%}$
10/02 08-09	3.74	3.46	3.16	2.57	4.22	1.65	3.14	1.80	4.44	3.92	3.05	2.04
10/02 09-10	3.81	3.52	3.21	2.62	4.30	1.67	3.21	1.82	3.98	3.63	3.31	1.63
10/02 10-11	3.88	3.58	3.27	2.66	4.38	1.70	3.28	2.13	4.50	4.36	3.43	2.24
10/02 11-12	3.85	3.53	3.23	2.63	4.33	1.68	3.26	2.27	4.42	4.10	3.42	2.56
10/02 12-13	3.84	3.49	3.19	2.60	4.29	1.66	3.26	2.48	4.12	3.95	3.45	2.63
10/02 13-14	3.85	3.48	3.18	2.59	4.28	1.66	3.27	2.54	4.55	4.33	3.57	2.71
10/02 14-15	4.00	3.63	3.32	2.70	4.46	1.73	3.40	2.62	4.75	4.52	3.44	2.80
10/02 15-16	4.11	3.76	3.44	2.80	4.62	1.79	3.50	2.86	5.00	4.80	3.62	2.94

Nat. Hazards Earth Syst. Sci. Discuss., https://doi.org/10.5194/nhess-2017-252
Manuscript under review for journal Nat. Hazards Earth Syst. Sci.
Discussion started: 22 September 2017

Natural Hazards and Earth System Sciences
Discussions

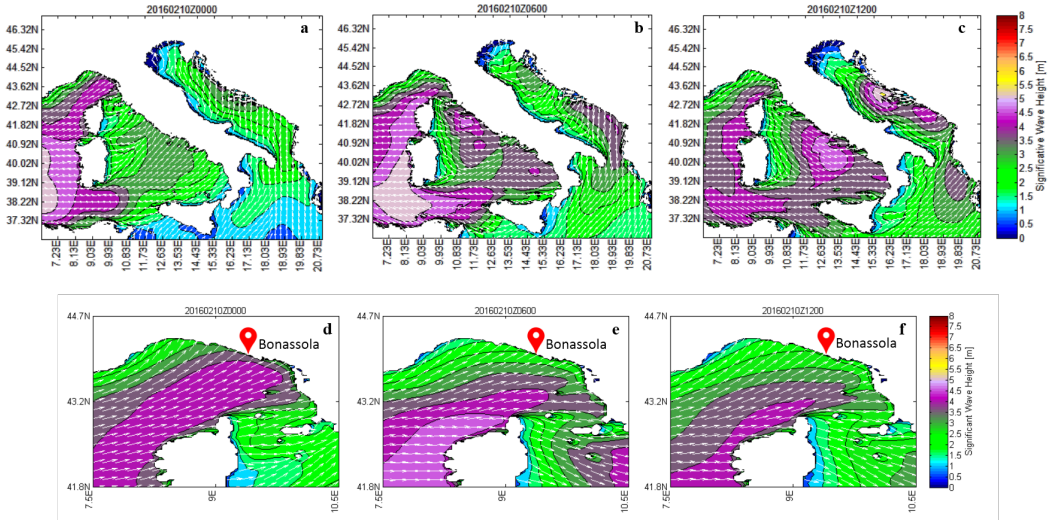

Figure 7. Ligurian Sea significant wave height (color maps) and direction (vector fields) in three moments of sea storm in February 2016. The maps are relative to WW3 model forecast on February 10th 2016 at: a) 00:00 UTM; b) 06:00 UTM; c) 12:00. Wave height isolines are at 0.5 m intervals.

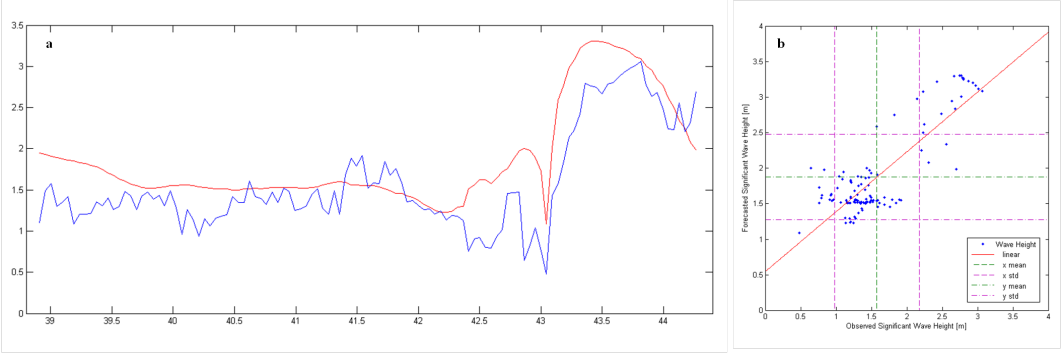

Figure 8. Matching between WW3 and Ku-band altimeter data from JASON-2 satellite pass. 44 cycle 280. a) Time series during the period from February 9th 2016 at 04:58:44 to 09th 2016 at 05:00:43. b) Scatter diagram between observed and simulated H_s [m]

Table 2 show the statistical measures used to describe the skill of the different run-up formulas. The comparison between observed and simulated $Ru_{2\%}$ is reported in Fig. 11. A first visual analysis shows that the simulated $Ru_{2\%}$ is almost always underestimated with respect to the observed one. In detail, the Holman (1986) equation gives the best matching with the observed values, with a mean RMSE of 0.40 m, the Mase (1989) equation gives a slightly lower matching, with RMSE of 0.70, and Stockdon et al. (2006) equation gives the less adherent results with a mean RMSE of 0.95 m. Conversely, the SPS values are in decreasing order, that is 0.91, 0.84 and 0.78, respectively. Fig. 12 shows the comparison among different run-up levels $Ru_{x\%}$ obtained by Mase (1989) and video camera observations. The results show a more uniform results of the numerical simulations

Nat. Hazards Earth Syst. Sci. Discuss., https://doi.org/10.5194/nhess-2017-252
Manuscript under review for journal Nat. Hazards Earth Syst. Sci.
Discussion started: 22 September 2017

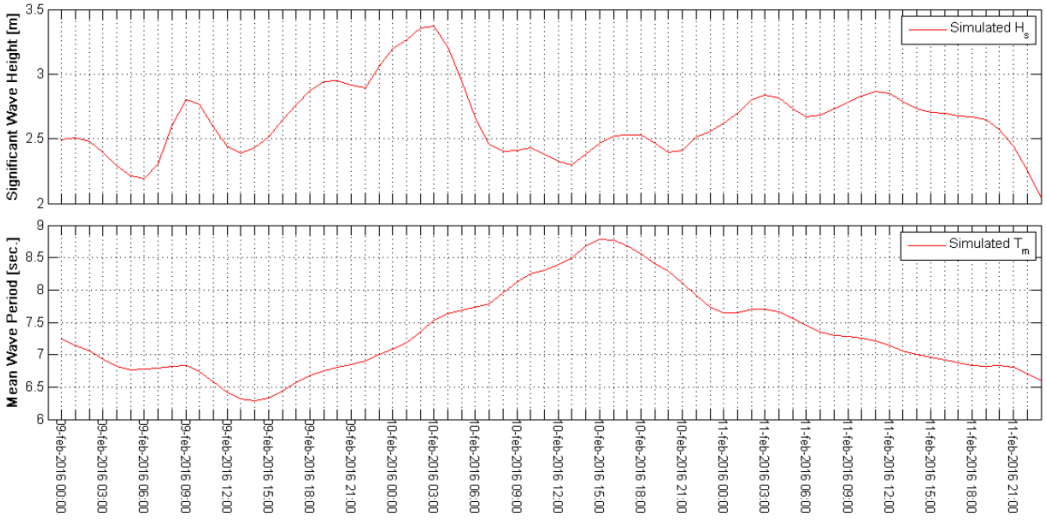

Figure 9. Forecasted significant wave height (H_s) and mean wave period (T_m) relative February 09th-11st 2016 sea storm at virtual buoy near Bonassola beach.

with respect to the observed ones, due to the lower time resolution of the WW3 model. Moreover, the results confirm that the best agreement is obtained for $Ru_{10\%}$, followed by $Ru_{33\%}$ and Ru_{max}, while the agreement for Ru_{mean} and $Ru_{2\%}$ is lower. These qualitative results are confirmed by the statistical indices reported in table 3, which can be synthesized using Melby Summary Performance Score (Melby et al. (2012)), an average of normalized RMSE, normalized BI and SI with an 0-1 scale, where 1 means no error. The values of this index is 0.94 for $Ru_{10\%}$, 0.86 for $Ru_{33\%}$ and 0.78 for Ru_{max}, while it is 0.84 for $Ru_{2\%}$ and 0.71 for Ru_{mean}.

5 Discussion

The comparison between the simulated and observed results of the beach run-up in the swash zone evidences that the wind-wave modelling chain gives also reliable results for simulations of the beach inundation in the time domain. The Summary Performance Score of Melby et al. (2012) was used to compare different run-up formulas in terms of their capability to follow the field run-up observations. The results of the run-up simulations obtained with Holman (1986) equation closely follow the video camera observations (SPS=0.91), with a good agreement with the ones of Melby et al. (2012) (SPS=0.84). The other formulations, for which the SPS value is similar to Holman's one, give satisfactory results, too (SPS=0.84 for Mase, SPS=0.78 for Stockdon). This circumstance proved that empirical wave run-up formulas are sufficiently accurate to be applied to Mediterranean beaches, and so they can be used in operational forecasting systems to evaluate the beach inundation levels.

Nat. Hazards Earth Syst. Sci. Discuss., https://doi.org/10.5194/nhess-2017-252
Manuscript under review for journal Nat. Hazards Earth Syst. Sci.
Discussion started: 22 September 2017

Natural Hazards and Earth System Sciences
Discussions

Table 3. Statistical error parameters obtained from the comparison among observed and simulated wave run-up levels.

	R	BI	SI	RMSE	NRMSE	RMS_P	BI_P	SI_P	SPS
Holman (1986) $Ru_{2\%}$	0.867	-0.075	0.098	0.410	0.097	0.903	0.925	0.903	0.910
Mase (1989) Ru_{mean}	0.669	-0.269	0.301	0.704	0.301	0.699	0.731	0.69	0.710
Mase (1989) $Ru_{33\%}$	0.519	0.083	0.174	0.431	0.17	0.83	0.917	0.826	0.856
Mase (1989) $Ru_{10\%}$	0.576	-0.047	0.061	0.209	0.061	0.939	0.953	0.939	0.943
Mase (1989) $Ru_{2\%}$	0.794	-0.154	0.167	0.704	0.167	0.833	0.847	0.833	0.838
Mase (1989) Ru_{max}	0.763	-0.025	0.057	0.255	0.057	0.943	0.975	0.432	0.783
Stockdon (2006) $Ru_{2\%}$	0.871	-0.217	0.225	0.949	0.225	0.051	0.783	0.775	0.778

Nat. Hazards Earth Syst. Sci. Discuss., https://doi.org/10.5194/nhess-2017-252
Manuscript under review for journal Nat. Hazards Earth Syst. Sci.
Discussion started: 22 September 2017

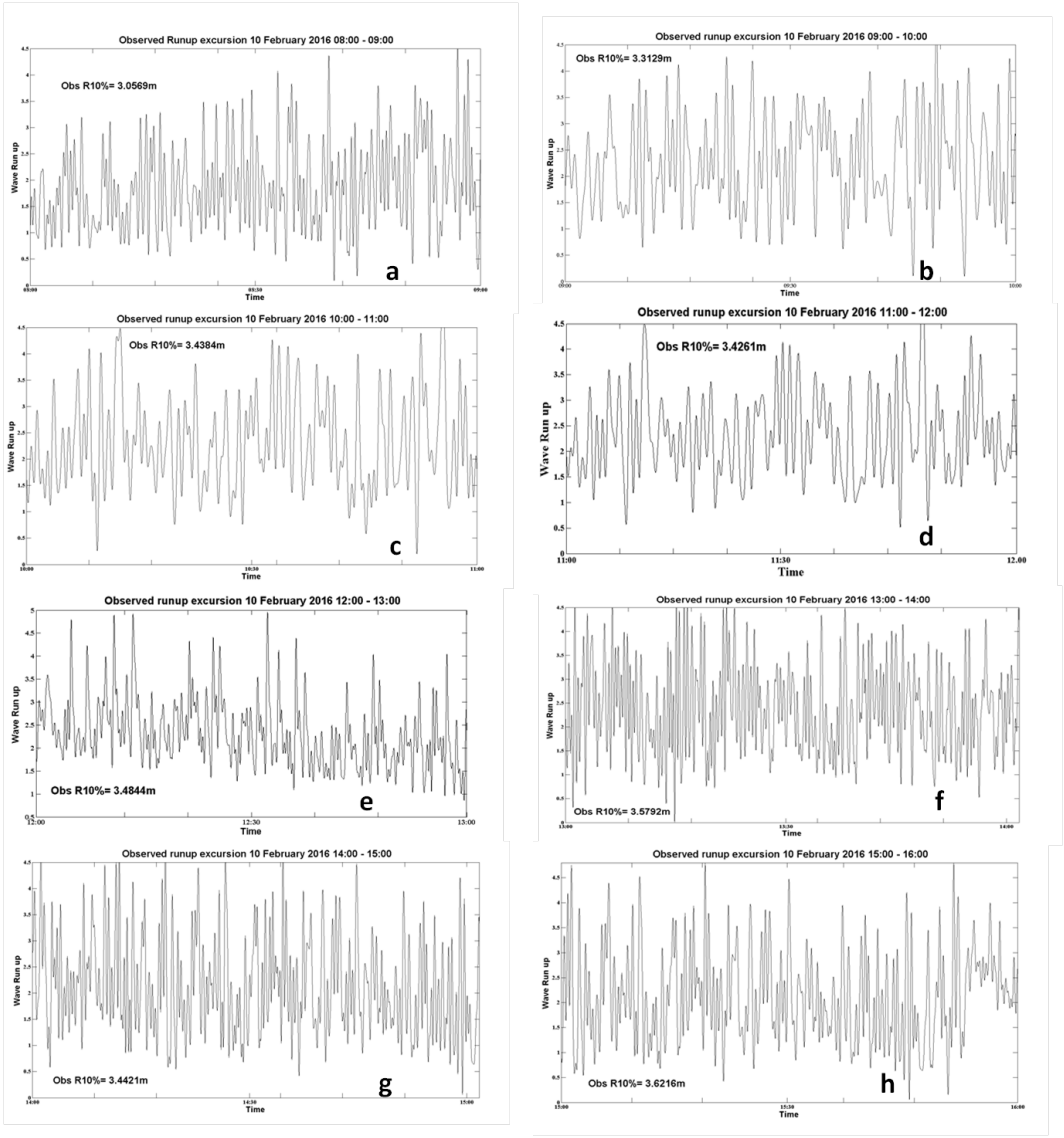

Figure 10. Wave run-up levels collected using pixel time stacks derived from video data of camera at Bonassola in February 10th 2016 at: (a) 8:00-9:00 UTC; (b) 9:00-10:00 UTC; (c) 10:00-11:00 UTC; (d) 11:00-12:00 UTC; (e) 12:00-13:00 UTC; (f) 13:00-14:00 UTC; (g) 14:00-15:00 UTC; (h) 15:00-16:00 UTC.

6 Conclusion and future directions

We configured a community and ad hoc developed numerical model chain to evaluate the beach inundation levels in a microtidal Mediterranean context. We used satellite altimeter data and video recorder cameras to setup a validation scheme of the proposed model chain, performed with reference to offshore waves and run-up level calculations. The satisfactory results of the

Nat. Hazards Earth Syst. Sci. Discuss., https://doi.org/10.5194/nhess-2017-252
Manuscript under review for journal Nat. Hazards Earth Syst. Sci.
Discussion started: 22 September 2017

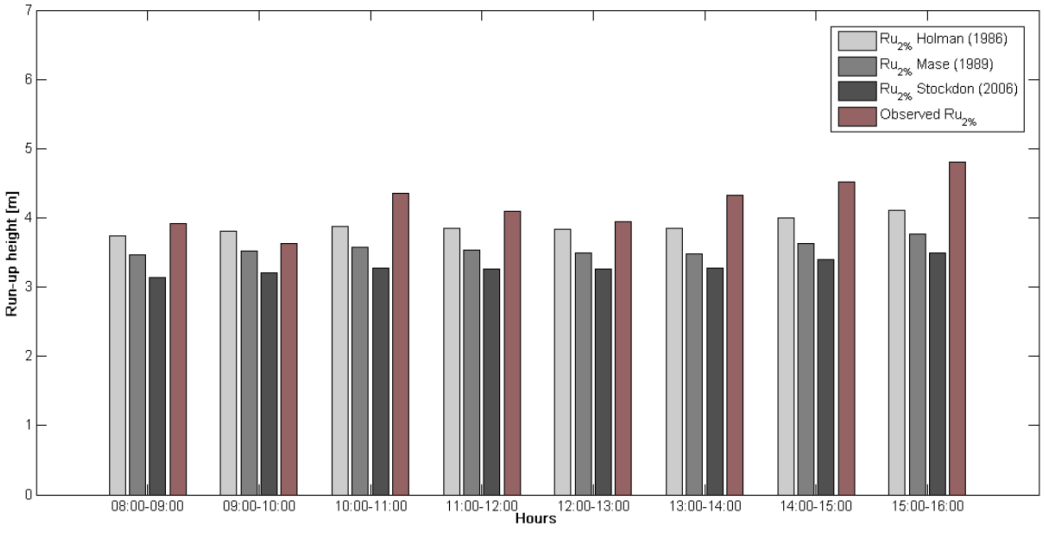

Figure 11. Comparison among observed and simulated $Ru_{2\%}$ with different formulas.

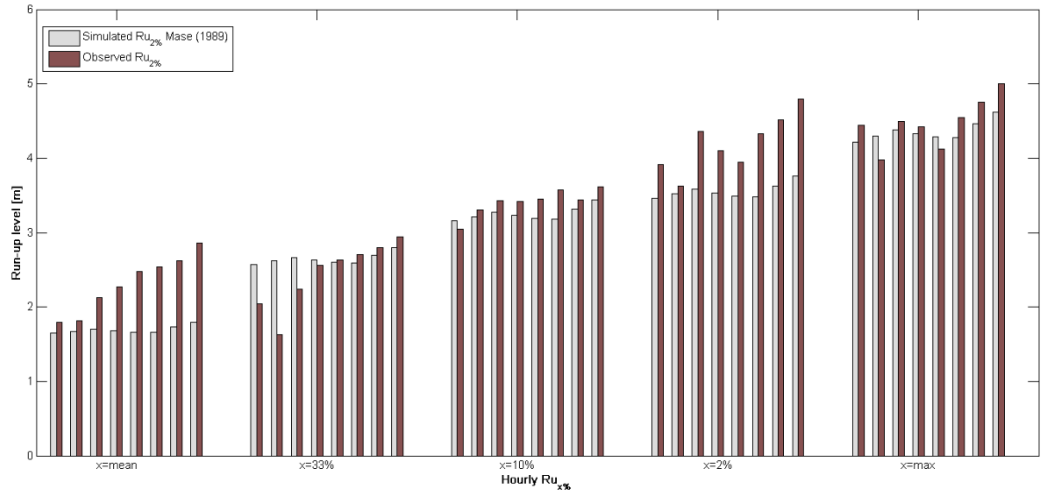

Figure 12. Comparison among different $Ru_{x\%}$ calculated with Mase (1989) equations and observations.

comparisons proved the ability of the model chain to be used as an operational forecasting system in coastal areas. In the next future, we will increase the resolution of the Wavewatch III domains in order to enable the run-up calculations for cliffs and coastal defence infrastructures. This improvement will need the implementation of the model chain using a cloud computing powered (Montella et al. (2015)) GPGPU based approach (Di Lauro et al. (2012)) in order to reduce the overall computational costs.

Nat. Hazards Earth Syst. Sci. Discuss., https://doi.org/10.5194/nhess-2017-252
Manuscript under review for journal Nat. Hazards Earth Syst. Sci.
Discussion started: 22 September 2017

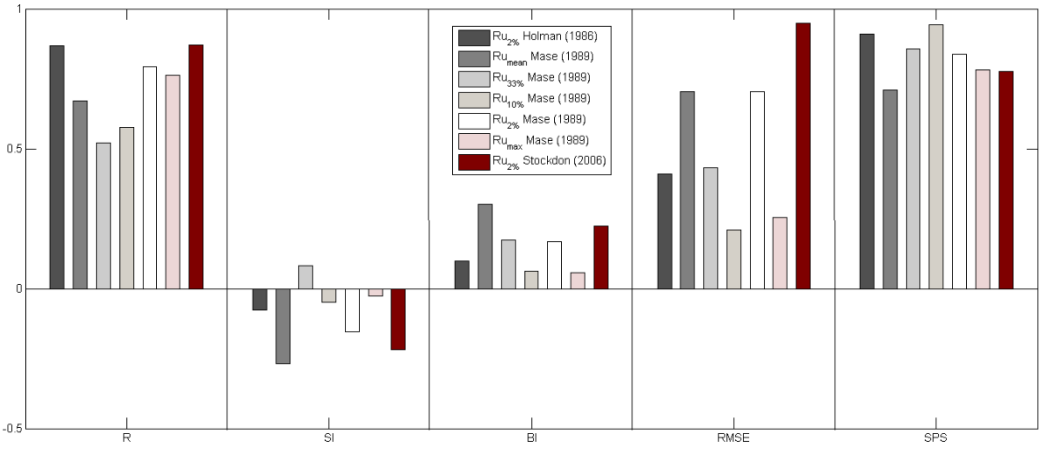

Figure 13. Bar diagram of statistical error parameters reported in Table 3.

Acknowledgements. The authors are grateful to the CCMMMA (*Campania Center for Marine and Atmospheric Monitoring and Modelling*, http://meteo.uniparthenope.it) that is the forecast service of the University of Napoli "*Parthenope*" for the real time monitoring and forecast of marine, weather and air quality conditions in the Mediterranean area. The CCMMMA provided the hardware and software resources for the offshore numerical simulations.

References

Aagaard, T. and Holm, J.: Digitization of wave run-up using video records, Journal of Coastal Research, pp. 547–551, 1989.

Airy, G. B.: Tides and waves, Encyclopaedia Metropolitana, 3, 1817–1845, 1841.

Ascione, I., Giunta, G., Mariani, P., Montella, R., and Riccio, A.: A grid computing based virtual laboratory for environmental simulations, Euro-Par 2006 Parallel Processing, pp. 1085–1094, 2006.

Aucelli, P. P. C., Di Paola, G., Incontri, P., Rizzo, A., Vilardo, G., Benassai, G., Buonocore, B., and Pappone, G.: Coastal inundation risk assessment due to subsidence and sea level rise in a Mediterranean alluvial plain (Volturno coastal plain–southern Italy), Estuarine, Coastal and Shelf Science, 2016.

Battjes, J. A.: Surf similarity, in: Coastal Engineering, Proceedings of 14th Conference on Coastal Engineering, Copenhagen, Denmark, 1974, vol. 14, pp. 466–480, ASCE, 1975.

Benassai, G. and Ascione, I.: Implementation and validation of wave watch III model offshore the coastlines of Southern Italy, in: Proceedings of 25th International Conference on Offshore Mechanics and Arctic Engineering, pp. 553–560, American Society of Mechanical Engineers, 2006a.

Benassai, G. and Ascione, I.: Implementation of WWIII wave model for the study of risk inundation on the coastlines of Campania, Italy, Environmental Problems in Coastal Regions VI: Including Oil Spill Studies, 88, 249, 2006b.

Benassai, G., Migliaccio, M., Montuori, A., and Ricchi, A.: Wave Simulations Through Sar Cosmo-Skymed Wind Retrieval and Verification with Buoy Data, in: Proceedings of the Twenty-second International Offshore and Polar Engineering Conference, International Society of Offshore and Polar Engineers, 2012.

Benassai, G., Migliaccio, M., and Montuori, A.: Sea wave numerical simulations with COSMO-SkyMed© SAR data, Journal of Coastal Research, 65, 660–665, 2013a.

Benassai, G., Montuori, A., Migliaccio, M., and Nunziata, F.: Sea wave modeling with X-band COSMO-SkyMed© SAR-derived wind field forcing and applications in coastal vulnerability assessment, Ocean Science, 9, 325, 2013b.

Benassai, G., Di Paola, G., and Aucelli, P. P. C.: Coastal risk assessment of a micro-tidal littoral plain in response to sea level rise, Ocean & Coastal Management, 104, 22–35, 2015a.

Benassai, G., Migliaccio, M., and Nunziata, F.: The use of COSMO-SkyMed© SAR data for coastal management, Journal of Marine Science and Technology, 20, 542–550, 2015b.

Benassai, G., Aucelli, P., Budillon, G., De Stefano, M., Di Luccio, D., Di Paola, G., Montella, R., Mucerino, L., Sica, M., and Pennetta, M.: Rip current evidence by hydrodynamic simulations, bathymetric surveys and UAV observation, Natural Hazards and Earth System Sciences, 17, 1493–1503, 2017.

Bertotti, L. and Cavaleri, L.: Wind and wave predictions in the Adriatic Sea, Journal of Marine Systems, 78, S227–S234, 2009.

Bidlot, J.-R., Holmes, D. J., Wittmann, P. A., Lalbeharry, R., and Chen, H. S.: Intercomparison of the performance of operational ocean wave forecasting systems with buoy data, Weather and Forecasting, 17, 287–310, 2002.

Brignone, M., Schiaffino, C. F., Isla, F. I., and Ferrari, M.: A system for beach video-monitoring: Beachkeeper plus, Computers & Geosciences, 49, 53–61, 2012.

Carratelli, E. P., Budillon, G., Dentale, F., Napoli, F., Reale, F., and Spulsi, G.: An experience in monitoring and integrating wind and wave data in the Campania Region, Bollettino di Geofisica Teorica ed Applicata, 48, 215–226, 2007.

Casella, E., Rovere, A., Pedroncini, A., Mucerino, L., Casella, M., Cusati, L. A., Vacchi, M., Ferrari, M., and Firpo, M.: Study of wave runup using numerical models and low-altitude aerial photogrammetry: A tool for coastal management, Estuarine, Coastal and Shelf Science, 149, 160–167, 2014.

Cavaleri, L. and Rizzoli, P. M.: Wind wave prediction in shallow water: Theory and applications, Journal of Geophysical Research: Oceans, 86, 10 961–10 973, 1981.

Di Lauro, R., Giannone, F., Ambrosio, L., and Montella, R.: Virtualizing general purpose GPUs for high performance cloud computing: an application to a fluid simulator, in: Parallel and Distributed Processing with Applications (ISPA), 2012 IEEE 10th International Symposium on, pp. 863–864, IEEE, 2012.

Di Paola, G., Aucelli, P. P. C., Benassai, G., and Rodríguez, G.: Coastal vulnerability to wave storms of Sele littoral plain (southern Italy), Natural hazards, 71, 1795–1819, 2014.

Didenkulova, I.: Marine natural hazards in coastal zone: observations, analysis and modelling (Plinius Medal Lecture), in: EGU General Assembly Conference Abstracts, vol. 12, p. 14748, 2010.

Didenkulova, I. and Pelinovsky, E.: Run-up of long waves on a beach: the influence of the incident wave form, Oceanology, 48, 1–6, 2008.

Didenkulova, I., Sergeeva, A., Pelinovsky, E., and Gurbatov, S.: Statistical estimates of characteristics of long-wave run-up on a beach, Izvestiya, Atmospheric and Oceanic Physics, 46, 530–532, 2010.

Dodd, N.: Numerical model of wave run-up, overtopping, and regeneration, Journal of Waterway, Port, Coastal, and Ocean Engineering, 124, 73–81, 1998.

Fenton, J. D. and McKee, W.: On calculating the lengths of water waves, Coastal Engineering, 14, 499–513, 1990.

Goda, Y.: On the methodology of selecting design wave height, in: Coastal Engineering Proceedings 1988, vol. 21, pp. 899–913, ASCE, 1989.

Holland, K. T. and Holman, R. A.: Video estimation of foreshore topography using trinocular stereo, Journal of Coastal Research, pp. 81–87, 1997.

Holman, R.: Extreme value statistics for wave run-up on a natural beach, Coastal Engineering, 9, 527–544, 1986.

Hubbard, M. E. and Dodd, N.: A 2D numerical model of wave run-up and overtopping, Coastal Engineering, 47, 1–26, 2002.

Hunt, I. A.: Design of sea-walls and breakwaters, Transactions of the American Society of Civil Engineers, 126, 542–570, 1959.

Johannessen, O. and Bjorgo, E.: Wind energy mapping of coastal zones by synthetic aperture radar (SAR) for siting potential windmill locations, International Journal of Remote Sensing, 21, 1781–1786, 2000.

Mase, H.: Random wave runup height on gentle slope, Journal of Waterway, Port, Coastal, and Ocean Engineering, 115, 649–661, 1989.

Melby, J., Caraballo-Nadal, N., and Kobayashi, N.: Wave runup prediction for flood mapping, Coastal Engineering Proceedings, 1, 79, 2012.

Mentaschi, L., Besio, G., Cassola, F., and Mazzino, A.: Developing and validating a forecast/hindcast system for the Mediterranean Sea, Journal of Coastal Research, 65, 1551–1556, 2013.

Montella, R., Giunta, G., and Riccio, A.: Using grid computing based components in on demand environmental data delivery, in: Proceedings of the second workshop on Use of P2P, GRID and agents for the development of content networks, pp. 81–86, ACM, 2007.

Montella, R., Agrillo, G., Mastrangelo, D., and Menna, M.: A globus toolkit 4 based instrument service for environmental data acquisition and distribution, in: Proceedings of the third international workshop on Use of P2P, grid and agents for the development of content networks, pp. 21–28, ACM, 2008.

Montella, R., Giunta, G., Laccetti, G., Lapegna, M., Palmieri, C., Ferraro, C., and Pelliccia, V.: Virtualizing CUDA Enabled GPGPUs on ARM Clusters., in: PPAM (2), pp. 3–14, 2015.

Montuori, A., Ricchi, A., Benassai, G., and Migliaccio, M.: Sea Wave Numerical Simulation and Verification in Tyrrhenian Costal area with X-Band COSMO-Skymed SAR data, in: Proceedings of the ESA, SOLAS & EGU Joint Conference Earth Observation for Ocean-Atmosphere Interactions Science, ESA-ESRIN, Frascati, Italy, vol. 703, ESA-SP, 2011.

Nunziata, F., Buono, A., Migliaccio, M., and Benassai, G.: Dual-polarimetric C-and X-band SAR data for coastline extraction, IEEE Journal of Selected Topics in Applied Earth Observations and Remote Sensing, 9, 4921–4928, 2016.

Ojeda, E., Ruessink, B., and Guillen, J.: Morphodynamic response of a two-barred beach to a shoreface nourishment, Coastal Engineering, 55, 1185–1196, 2008.

Pham, Q., Malik, T., Foster, I. T., Di Lauro, R., and Montella, R.: SOLE: Linking Research Papers with Science Objects., in: IPAW, pp. 203–208, Springer, 2012.

Reale, F., Dentale, F., Carratelli, E. P., and Torrisi, L.: Remote sensing of small-scale storm variations in coastal seas, Journal of Coastal Research, 30, 130–141, 2014.

Rusu, L., Bernardino, M., and Guedes Soares, C.: Wind and wave modelling in the Black Sea, Journal of Operational Oceanography, 7, 5–20, 2014.

Shore Protection Manual, .: Department of the Army, Waterways Experiment Station, Corps of Engineers, Coastal Engineering Researcher Center, 2, 1984.

Skamarock, W. C., Klemp, J. B., and Dudhia, J.: Prototypes for the WRF (Weather Research and Forecasting) model, in: Preprints, Ninth Conf. Mesoscale Processes, J11–J15, Amer. Meteorol. Soc., Fort Lauderdale, FL, 2001.

Stockdon, H. F., Holman, R. A., Howd, P. A., and Sallenger, A. H.: Empirical parameterization of setup, swash, and runup, Coastal engineering, 53, 573–588, 2006.

Takewaka, S. and Nakamura, T.: Surf zone imaging with a moored video system, in: Proceedings of the International Conference on Coastal Engineering 2000, pp. 1211–1216, ASCE, 2001.

Tolman, H. L. and Chalikov, D.: Source terms in a third-generation wind wave model, Journal of Physical Oceanography, 26, 2497–2518, 1996.

Tolman, H. L. et al.: User manual and system documentation of WAVEWATCH III TM version 3.14, Technical note, MMAB Contribution, 276, 220, 2009.

Zhang, S. and Zhang, C.: Application of ridgelet transform to wave direction estimation, in: Image and Signal Processing, 2008. CISP'08. Congress on, vol. 2, pp. 690–693, IEEE, 2008.